Electronic Supplementary Material (ESI) for Chemical Communications.

Unprecedented Self-assembled Architectures of Surface Active Ionic Liquids in Aqueous Medium

Gurbir Singh,[a] Manvir Kaur,[a] Markus Drechsler,[b] Tejwant Singh Kang[a,]*

[a] *Department of Chemistry, UGC-centre for Advance Studies – II, Guru Nanak Dev University, Amritsar, 143005, India.*

[b] *Bavarian Polymer Institute (BPI), KeyLab Electron and Optical Microscopy, University Bayreuth, 95447 Bayreuth, Germany*

Supporting Information

**To whom correspondence should be addressed:*

e-mail: tejwantsinghkang@gmail.com; tejwant.chem@gmail.com Tel: +91-183-2258802-Ext-3207

Annexure S1.

Materials: Benzimidazole (>98) 1-bromobutane (>99), 1-bromododecane (>97), dodecane-1-ol (>98), 1-aminododecane (>99), bromoacetic acid (>99), bromoacetyl bromide (>99), *p*-toluene sulphonic acid (>99) and tetrahydrofuran (anhydrous, >99) were obtained from Sigma and used without further purification. Hexane, ethyl acetate, chloroform, methanol, diethyl ether, dichloromethane, and acetone (AR Grade) has been procured from SD fine chemicals Ltd, Mumbai, India. All the measurements were performed in the Millipore water having resistivity of 18Ω. A Detailed description of the procedure followed for the synthesis of SAILs and their characterization using the NMR and Mass spectrophotometer is given in annexure S2.

Methods: Data Physics DCAT II automated tensiometer employing the Wilhelmy plate method was used for performing the surface tension measurements at 298.15 K. The Experiments were repeated for three times and values of surface tension were found to be within the accuracy of ±0.1 mN m^{-1}. The temperature was controlled using the water circulating thermostat to an accuracy of ±0.1 K. The specific conductance of the ionic liquid aqueous solutions was measured at 298.15 K employing digital conductivity meter (Systronics 308) having a unit cell constant. The temperature of the measurement was controlled using a thermostat within ±0.1 K. Measurements were done in triplicate within uncertainty of less than 3 %. Fluorescence of ionic liquid aqueous solutions was recorded in the range 295 to 550 nm using Perkin Elmer LS-55 spectrophotometer by exciting the sample at a wavelength of 280 nm at 298.15 K. Spectra were collected by sequential additions of stock solution of respective IL to the fixed volume of water in quartz cuvette of path length 1.0 cm using excitation and emission slit width of 2.5 nm. Temperature was controlled by Julabo water thermostat assembly within ±0.1 K. Isothermal titration calorimetric measurements were performed on MicroCal ITC200 micro-calorimeter. An Automatic titration was performed within the instrument by adding 2 μL of concentrated stock solution of IL from an instrument controlled Hamilton syringe having a volume capacity of 40 μL into the cell having 200 μL of water with continuous stirring at 500 rpm. The temperature of the instrument was controlled by built in temperature controller with an accuracy of ±0.1K. Turbidity measurements were performed using Oakton T-100 handheld turbidity meter at 298.15 K. A concentrated stock solution was titrated to the turbidity vessel containing 10 mL of water. The instrument was calibrated and checked before making sample measurements using the standard solutions of 800, 100, 20, 0.02 NTU. Zeta Sizer Nano ZS (Malvern Instruments) light

scattering apparatus equipped with a built-in temperature controller having an accuracy of ±0.1 K is used for performing the dynamic light scattering (DLS) measurements at 298.15 K. A quartz cuvette of 1 cm path length was used for holding the sample. Backscattering mode at a scattering angle of 173◦ was used for performing all the measurements. To avoid interference from dust particles all the samples were filtered before doing the measurements using Acrodisc syringe filters (0.45μm). The data is analyzed using standard algorithms and is reported with an uncertainty of less than 8%. For cryo-TEM studies, a 2 μL droplet of dispersion was put on a lacey carbon-coated copper grid, where most of the liquid was removed with blotting paper in a temperature- and humidity controlled freezing unit (Leica EM GP, Germany), leaving a thin film stretched over the lace. The specimens were instantly vitrified by rapid immersion into liquid ethane and cooled to approximately 90 K. The temperature and the humidity as monitored and kept constant in the environmental chamber during all of the sample preparation steps. After freezing, the specimen was inserted into a cryo-transfer holder (CT3500, Gatan, Germany) and transferred to a Zeiss / LEO EM922 OMEGA EFTEM (Carl Zeiss Mikroskopie, Germany). Examinations were carried out at temperatures around 95 K. Zero-loss filtered micrographs (E ~ 0 eV) were recorded under reduced dose conditions (100-1000 e/nm2 by a CCD digital camera (Ultrascan 1000, Gatan, Germany) and analyzed using GMS 1.8 software (Gatan, Germany). ^{1}H NMR and 2D $^{1}H-{}^{1}H$ NOESY experiments were performed on a Bruker Ascend 500 spectrometer (AVANCE III HD console) with water suppression in a 10% D_2O- 90% H_2O mixture using a 5 mm BBO (broad-band observe) double-channel probe equipped with z-gradients. Phase sensitive ^{1}H homonuclear 2D NOESY NMR experiment was recorded with experimental parameters: FID size 2048:F2 and 128:F1, numbers of scan: 32, mixing time of 500 ms and the data obtained was processed using Topspin NMR software. Differential scanning calorimetry studies have been performed on METTLER TOLEDO Differential scanning calorimeter DSC 3 instrument equipped with a robust and versatile DSC sensor with 56 thermocouples. Melting point of the investigated SAILs were analyzed by scanning the samples in the temperature range of 15-125 ^{o}C at the heating rate of 2 ^{o}C min^{-1} under N_2 environment. DSC curves for aqueous solutions of SAILs at twice their *cac* was recorded using aluminum crucible over the temperature range of 3-70 ^{o}C at a heating rate of 2 ^{o}C min^{-1} under N_2 environment. Thermal stability of the SAILs was investigated by employing themrogravimetric analysis (TGA) performed on TGA/SDT A851 Mettler Toledo thermogravimeter analyzer under

N_2 atmosphere at a heating rate of 5 ^oC min^{-1} in the temperature range of 25 to 600 ^oC. Purity of the synthesized SAILs has been established using the gas chromatography mass spectroscopy (GC-MS), which was performed on the SHIMADZU's GCMS TQ 8040 equipped with RTX- 5 column (30m length, 0.5 μm thickness and 0.25mm diameter) at a column flow rate of 1 mL min^{-1} using helium as carrier gas. The temperature program started at 40^0C and held for 3 min, then to 90^0C at the rate of 15^0C /min, then held for 10 min before measurements.

Annexure S2.

Synthesis and characterization of the $[C_4C_{12}bzm][Cl]$ and $[C_4C_{12}Xbzm][Cl]$ ILs.

N-butylbenzimidazole was prepared by following the procedure given in the literature with slight modifications [1]. Solution of benzimidazole (**1**; 50 mmol, 5.91 g) in THF (50mL) was added dropwise to a suspension of oil-free sodium hydride (100 mmol, 2.4 g) in THF (50 mL) under nitrogen atmosphere at room temperature. When the evolution of hydrogen gas was ceased from the above suspention, 1-bromobutane (**2**; 50 mmol, 6.85 g) in THF (100 mL) was dropwise added to it and the mixture was stirred at 60 °C for overnight. Solvent was removed using rotary evaporator and a yellow solution was obtained to which H_2O was added and the product was extracted with dichloromethane (50 mL × 3). The dichloromethane layer was dried over sodium sulphate and after removal of dichloromethane, an oily yellow liquid was obtained. *N*-butylbenzimidazole as colorless liquid (**3**; 7.2 g, 82.6% yield) was obtained after further purifying the yellow liquid using column chromatogrphy (EtOAc/*n*-hexane = 1/20). The two other intermediates dodecyl 2-chloroacetate and 2-chloro-*N*-dodecylacetamide required for the synthesis of SAILs were synthesized in similar manner as prepared by our own group in the previous reports [2,3].

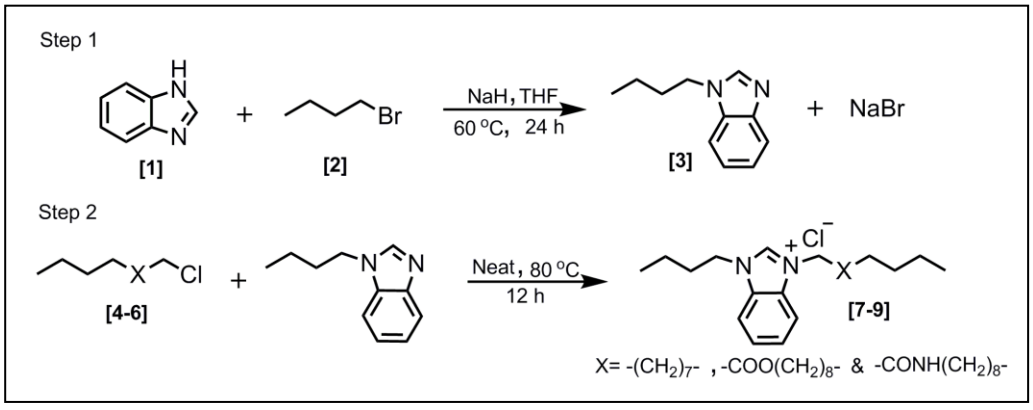

The resulting intermediate n-butylbenzimidazole (**3**; 10 mmol, 1.74 g) was allowed to react with the 1-chlorododecane (**4**, 10 mmol, 2.04 g), dodecyl 2-chloroacetate (**5**; 10 mmol, 2.62g) and 2-chloro-*N*-dodecylacetamide (6; 10 mmol, 2.61 g) at 80°C for 12 hours. The progress of the reaction was monitored by observing disappearance of the spot corresponding to n-butylbenzimidazole on the TLC plate in 30% ethyl acetate/hexane solvent mixture. Then the crude reaction mixture was cooled to 25 °C washed three times each with 50 mL of diethyl ether and hexane. The product obtained was cold precipitated using acetone and dried under vacuum using rotary evaporator to get pure benzimidazolium based Surface active ionic liquid (SAILs) (**7-9**). SAILS after above purification step were obtained as white powder at room temperature and their respective % yields are $[C_4C_{12}bzm][Cl]$ (**7;** 3.2 g, 84.6% yield); $[C_4C_{12}Abzm][Cl]$ (**8;** 3.9 g, 89.4% yield); $[C_4C_{12}Ebzm][Cl]$ (**9;** 4.1g, 94.0 % yield). The molecular structures and purity of synthesized SAILs were confirmed by ^1H , ^{13}C/DEPT NMR and mass spectrometry. ^1H , ^{13}C/DEPT NMR spectra were recorded on Brüker Ascend 500 spectrometer (AVANCE III HD console) in $CDCl_3$ as solvent. Waters Q-ToF micromass equipment having ESI as the ion source was used to record high resolution mass spectra of SAILs. Further the purity of SAILs has been established by performing gas chromatography mass spectroscopy (GCMS).

^{1}H NMR and mass spectroscopy data for synthesized ILSs:

N-methylbenzimidazole, C_4bzm: ^1H NMR (500 MHz, $CDCl_3$, δ-ppm) 0.997 (t, 3H, N−CH_2−CH_2−CH_2−C*H*$_3$), 1.35 (m, 2H,−N−CH_2−CH_2−C*H*$_2$−CH_3), 1.86 (m, 2H,−N−CH_2−C*H*$_2$−CH_2−CH_3), 4.16 (m, 2H,−N−C*H*$_2$−CH_2−CH_2−CH_3), 7.29 (m, 1H, butyl−N−C=CH−CH=C*H*−CH=C−N=C−), 7.32 (m, 1H, butyl−N−C=CH−C*H*=CH−CH=C−N=C−), 7.41 (m, 1H, butyl−N−C=CH−CH=CH−C*H*=C−N=C−), 7.80 (m, 1H, butyl−N−C=C*H*−CH=CH−CH=C−N=C−), 7.88 (s, 1H, −N−C*H*−N^+−).

[C_4C_{12}bzm][Cl]: ^1H NMR (500 MHz, $CDCl_3$, δ-ppm) 0.876 (t, 3H, dodecyl terminal-C*H*$_3$), 0.997 (t, 3H, N−CH_2−CH_2−CH_2−C*H*$_3$), 1.238 (br s, 14H, (-C*H*$_2$-)$_7$), 1.348 (br m, 2H, N^+−CH_2−CH_2−CH_2−C*H*$_2$−), 1.421 (br m, 2H,−N^+−CH_2−CH_2−C*H*$_2$−CH_2−), 1.466 (m, 2H,−N−CH_2−CH_2−C*H*$_2$−CH_3), 2.032 (m, 2H,−N−CH_2−C*H*$_2$−CH_2−CH_3), 2.061 (m, 2H,−N^+−CH_2−C*H*$_2$−CH_2−CH_2−), 4.637 (m, 2H,−N−C*H*$_2$−CH_2−CH_2−CH_3), 4.657 (m, 2H,−N^+−C*H*$_2$−CH_2−CH_2−CH_2−), 7.655 (m, 1H, −N−C=C*H*−CH=CH−CH=C−N^+−), 7.667 (m, 1H, −N−C=CH−C*H*=CH−CH=C−N^+−), 7.70 (m, 1H, −N−C=CH−CH=C*H*−CH=C−N^+−), 7.713 (m, 1H, −N−C=CH−CH=CH−C*H*=C−N^+−), 11.536 (s, 1H, −N−C*H*−N^+−).

^{13}C NMR ($CDCl_3$) δ ppm: 13.52 (-N−CH_2−CH_2−CH_2−*C*H_3), 14.10 (−CH2−CH_2−*C*H_3), 19.84(−N−CH_2−CH_2−*C*H_2−CH_3), 22.66 (−CH2−*C*H_2−CH_3), 26.56 (−N^+−CH_2−CH_2−*C*H_2−CH_2−), 29.04−29.56(chain (−C*H*$_2$−)$_7$), 31.40 (−*C*H2−CH_2−CH_3), 31.88 (-N−CH_2−*C*H_2−CH_2−CH_3), 47.43 (-N−*C*H_2−CH_2−CH_2−*C*H_3), 47.70 (−N^+−*C*H_2−CH_2−CH_2−), 113.05 (−N−C=*C*H−CH=CH−*C*H=C−N^+−), 126.96 (−N−C=CH−*C*H=*C*H−CH=C−N^+−), 131.38 (−N−*C*=CH−CH=CH−CH=*C*−N^+−), 143.73 (s, 1H, −N−*C*H−N^+−).

^{13}C/DEPT NMR ($CDCl_3$) δ ppm: 13.52 (+ve,−N−CH_2−CH_2−CH_2−*C*H_3), 14.10 (+ve,−CH2−CH_2−*C*H_3), 19.84 (-ve, −N−CH_2−CH_2−*C*H_2−CH_3), 22.66 (-ve, −CH2−*C*H_2−CH_3), 26.56 (-ve, −N^+−CH_2−CH_2−*C*H_2−CH_2−), 29.04−29.56(-ve, chain (−C*H*$_2$−)$_7$), 31.40 (-ve, −*C*H2−CH_2−CH_3), 31.88 (-ve,−N−CH_2−*C*H_2−CH_2−CH_3), 47.43 (-ve, -N−*C*H_2−CH_2−CH_2−CH_3), 47.70 (–ve, –N^+−*C*H_2−CH_2−CH_2−), 113.05 (+ve,−N−C=*C*H−CH=CH−*C*H=C−N^+−), 126.96 (+ve, −N−C=CH−*C*H=*C*H−CH=C−N^+−), 143.73 (+ve, −N−*C*H−N^+−). ESI-HRMS positive ions m/z (for $C_{23}H_{39}N_2^+$): 343.3046, 343.3125.

[C_4C_{12}Abzm][Cl]: ^{1}H NMR (500 MHz, $CDCl_3$, δ-ppm) 0.876 (t, 3H, terminal-C*H*$_3$), 1.012 (t, 3H,−N−CH_2−CH_2−CH_2 −C*H*$_3$), 1.218 (br s, 18H, (-C*H*$_2$-)$_9$), 1.478 (m, 2H,−N−CH_2−CH_2−C*H*$_2$−CH_3), 1.546 (m, 2H,−CO−NH−CH_2−C*H*$_2$−CH_2−CH_2−), 2.043 (m, 2H,−N−CH_2−C*H*$_2$−CH_2−C*H*$_3$), 3.20 (m, 2H,−CO−NH−C*H*$_2$−CH_2−CH_2−), 4.447 (t, 2H,−N−C*H*$_2$−CH_2−CH_2−CH_3), 5.664 (s, 2H,−N^+−C*H*$_2$−CO−NH−CH_2−), 7.636 (m, 1H, −N−C=C*H*−CH=CH−CH=C−N^+−), 7.636 (m, 1H, −N−C=CH−C*H*=CH−CH=C−N^+−), 7.636 (m, 1H, −N−C=CH−CH=C*H*−CH=C−N^+−), 8.059 (m, 1H, −N−C=CH−CH=CH−C*H*=C−N^+−), 9.290 (t, 2H,−N^+−CH_2−CO−N*H*−CH_2−), 10.658 (s, 1H, −N−C*H*−N^+−).

^{13}C NMR ($CDCl_3$) δ ppm: 13.45 (-N−CH_2−CH_2−CH_2−*C*H_3), 14.12 (−CH2−*C*H_2−*C*H_3), 19.85 (−N−CH_2−CH_2−*C*H_2−CH_3), 22.68 (−CH2−*C*H_2−CH_3), 27.06 (−N^+−CH_2−CONH2−CH_2−CH_2−*C*H_2−), 29.13−29.62 (chain (−C*H*$_2$−)$_7$), 31.08 (−*C*H2−CH_2−CH_3), 31.91 (-N−CH_2−*C*H_2−CH_2−CH_3), 40.09 (−N^+−CH_2−CONH$_2$−*C*H_2−CH_2−CH_2−), 47.53 (-N−*C*H_2−CH_2−CH_2−*C*H_3), 49.94 (−N^+−*C*H_2−CONH$_2$−CH_2−CH_2−), 112.23 (−N−C=*C*H−CH=CH−CH=C−N^+−), 114.88 (−N−C=CH−CH=CH−*C*H=C−N^+−), 127.15 (−N−C=CH−*C*H=CH−CH=C−N^+−), 127.49 (−N−C=CH−CH=*C*H−CH=C−N^+−), 130.86 (−N−*C*=CH−CH=CH−CH=C−N^+−), 132.14 (−N−C=CH−CH=CH−CH=*C*−N^+−), 142.65 (s, 1H, −N−*C*H−N^+−),164.26 (−N^+−CH_2−*C*ONH$_2$−CH_2−).

^{13}C/DEPT NMR ($CDCl_3$) δ ppm: 13.45 (+ve, -N−CH_2−CH_2−CH_2−*C*H_3), 14.12 (+ve,−CH2−*C*H_2−*C*H_3), 19.85 (-ve, N−CH_2−CH_2−*C*H_2−CH_3), 22.68 (-ve,−CH2−*C*H_2−CH_3), 27.06 (-ve,−N^+−CH_2−

CONH2−CH_2−CH_2−*C*H_2−), 29.13−29.62 (-ve, chain (−C*H*$_2$−)$_7$), 31.08 (-ve, −*C*H2−CH_2−CH_3), 31.91 (-ve,−N−CH_2−*C*H_2−CH_2−CH_3), 40.09 (-ve,−N^+−CH_2−$CONH_2$−*C*H_2−CH_2−CH_2−), 47.53 (-ve,−N−*C*H_2−CH_2−CH_2−*C*H_3), 49.94 (-ve,−N^+−*C*H_2−$CONH_2$−CH_2−CH_2−), 112.23 (+ve, N−C=*C*H−CH=CH−CH=C−N^+−), 114.88 (+ve, N−C=CH−CH=CH−*C*H=C−N^+−), 127.15 (+ve, N−C=CH−*C*H=CH−CH=C−N^+−), 127.49 (+ve,−N−C=CH−CH=*C*H−CH=C−N^+−), 142.65 (+ve, −N−*C*H−N^+−). ESI-HRMS positive ions m/z (for $C_{23}H_{39}N_2^+$): 400.2997, 401.3017.

[C_4C_{12}Ebzm][Cl]: ^{1}H NMR (500 MHz, $CDCl_3$, δ-ppm) 0.883 (t, 3H, terminal-C*H*$_3$), 1.009 (t, 3H, N−CH_2−CH_2−CH_2 −C*H*$_3$), 1.262 (br s, 18H, (-C*H*$_2$-)$_9$), 1.480 (m, 2H,−N−CH_2−CH_2−C*H*$_2$−CH_3), 1.670 (m, 2H,−COO−CH_2−C*H*$_2$−CH_2−CH_2−), 2.065 (m, 2H,−N−CH_2−C*H*$_2$−CH_2−C*H*$_3$), 4.217 (t, 2H,−COO−C*H*$_2$−CH_2−CH_2−), 4.576 (t, 2H,−N−C*H*$_2$−CH_2−CH_2−C*H*$_3$), 5.766 (s, 2H,−N^+−C*H*$_2$−COO−CH_2−), 7.582 (m, 1H, −N−C=C*H*−CH=CH−CH=C−N^+−), 7.654 (m, 1H, −N−C=CH−C*H*=CH−CH=C−N^+−), 7.676 (m, 1H, −N−C=CH−CH=C*H*−CH=C−N^+−), 7.728 (m, 1H, −N−C=CH−CH=CH−C*H*=C−N^+−), 11.536 (s, 1H, −N−C*H*−N^+−).

^{13}C NMR ($CDCl_3$) δ ppm: 13.46 (-N−CH_2−CH_2−CH_2−*C*H_3), 14.10 (−CH2−*C*H_2−*C*H_3), 19.89 (-N−CH_2−CH_2−*C*H_2−CH_3), 22.67 (−CH2−*C*H_2−CH_3), 25.71 (-N^+−CH_2−COO−CH_2−CH_2−*C*H_2−), 28.35 29.85 (chain (−C*H*$_2$−)$_7$), 31.90 (−*C*H2−CH_2−CH_3), 34.38 (-N−CH_2−*C*H_2−CH_2−CH_3), 47.70 (-N−*C*H_2−CH_2−CH_2−*C*H_3), 47.87 (-N^+−*C*H_2−COO−CH_2−CH_2−), 67.80 (-N^+−CH_2−COO−*C*H_2−CH_2−CH_2−), 112.98 (-N−C=*C*H−CH=CH−CH=C−N^+−), 113.04 (-N−C=CH−CH=CH−*C*H=C−N^+−), 127.19 (-N−C=CH−*C*H=CH−CH=C−N^+−), 127.40 (-N−C=CH−CH=*C*H−CH=C−N^+−), 131.00 (-N−*C*=CH−CH=CH−CH=C−N^+−), 131.74 (-N−C=CH−CH=CH−CH=*C*−N^+−), 144.44 (s, 1H, −N−*C*H−N^+−),166.91 (-N^+−CH_2−*C*OO−CH_2-).

^{13}C/DEPT NMR ($CDCl_3$) δ ppm: 13.46 (+ve, -N−CH_2−CH_2−CH_2−*C*H_3), 14.10 (+ve, −CH2−CH_2−*C*H_3), 19.89 (-ve,−N−CH_2−CH_2−*C*H_2−CH_3), 22.67 (-ve,−CH2−*C*H_2−CH_3), 25.71 (-ve,−N^+−CH_2−COO−CH_2−CH_2−*C*H_2−), 28.35−29.85 (-ve, chain (−*C*H_2−)$_7$), 31.90 (-ve,−*C*H2−CH_2−CH_3), 34.38 (-ve,−N−CH_2−*C*H_2−CH_2−CH_3), 47.70 (-ve,−N−*C*H_2−CH_2−CH_2−*C*H_3), 47.87 (-ve,−N^+−*C*H_2−COO−CH_2−CH_2−), 67.80 (-ve,−N^+−CH_2−COO−*C*H_2−CH_2−CH_2−), 112.98 (+ve,−N−C=*C*H−CH=CH−CH=C−N^+−), 113.04 (+ve,−N−C=CH−CH=CH−*C*H=C−N^+−), 127.19 (+ve,−N−C=CH−*C*H=CH−CH=C−N^+−), 127.40 (+ve,−N−C=CH−CH=*C*H−CH=C−N^+−), 144.44 (+ve, −N−*C*H−N^+−).

ESI-HRMS positive ions m/z (for $C_{23}H_{39}N_2^+$): 401.3425, 402.3450.

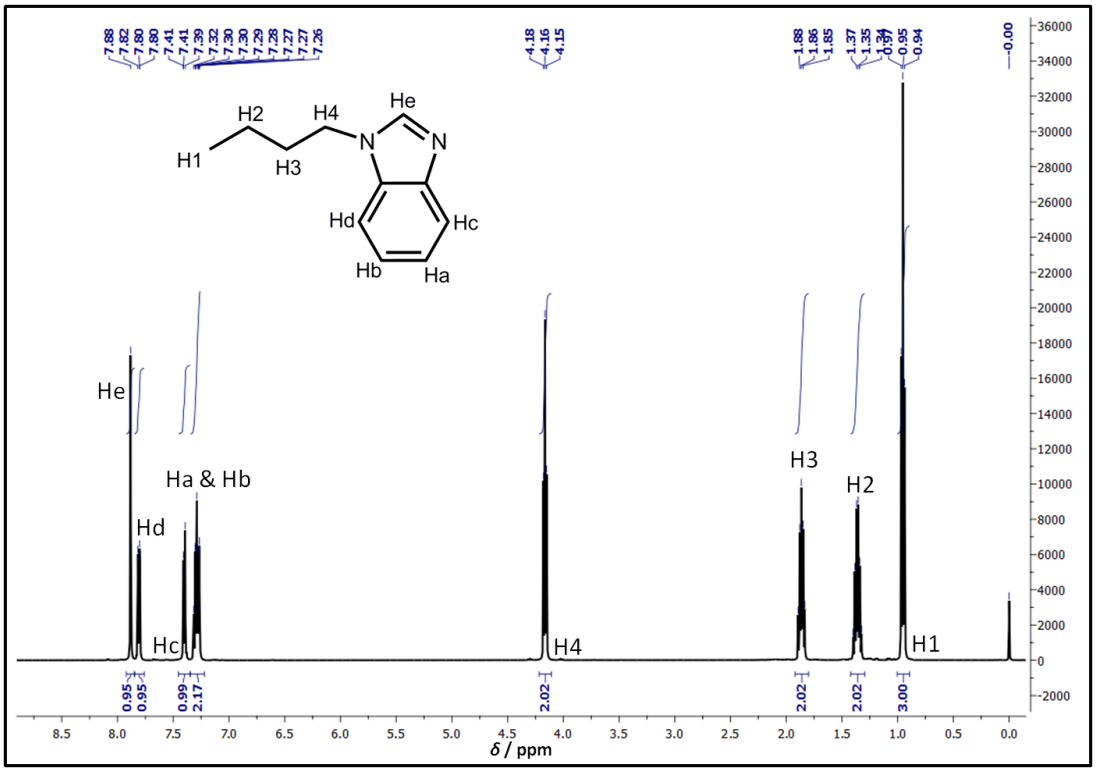

Fig. S1: Labeled ^{1}H NMR spectra of intermediate [3] formed in step 1 of synthesis along with its molecular structure.

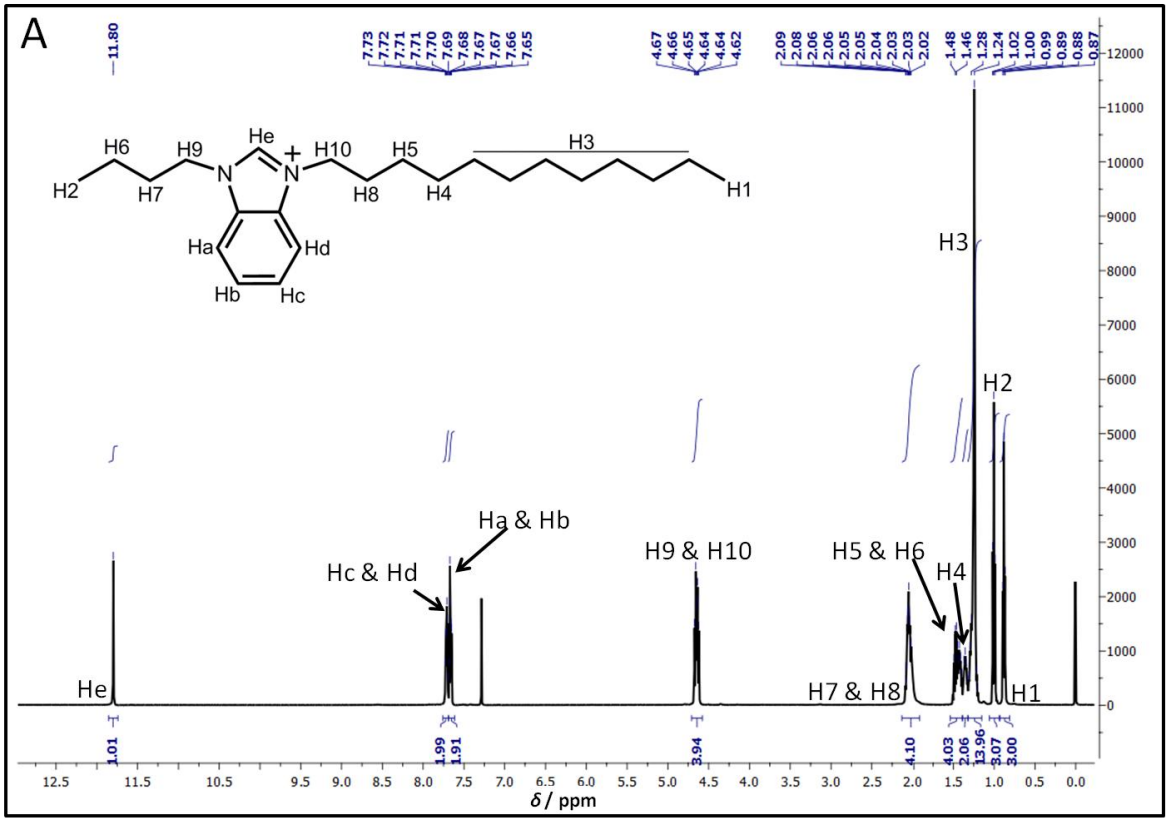

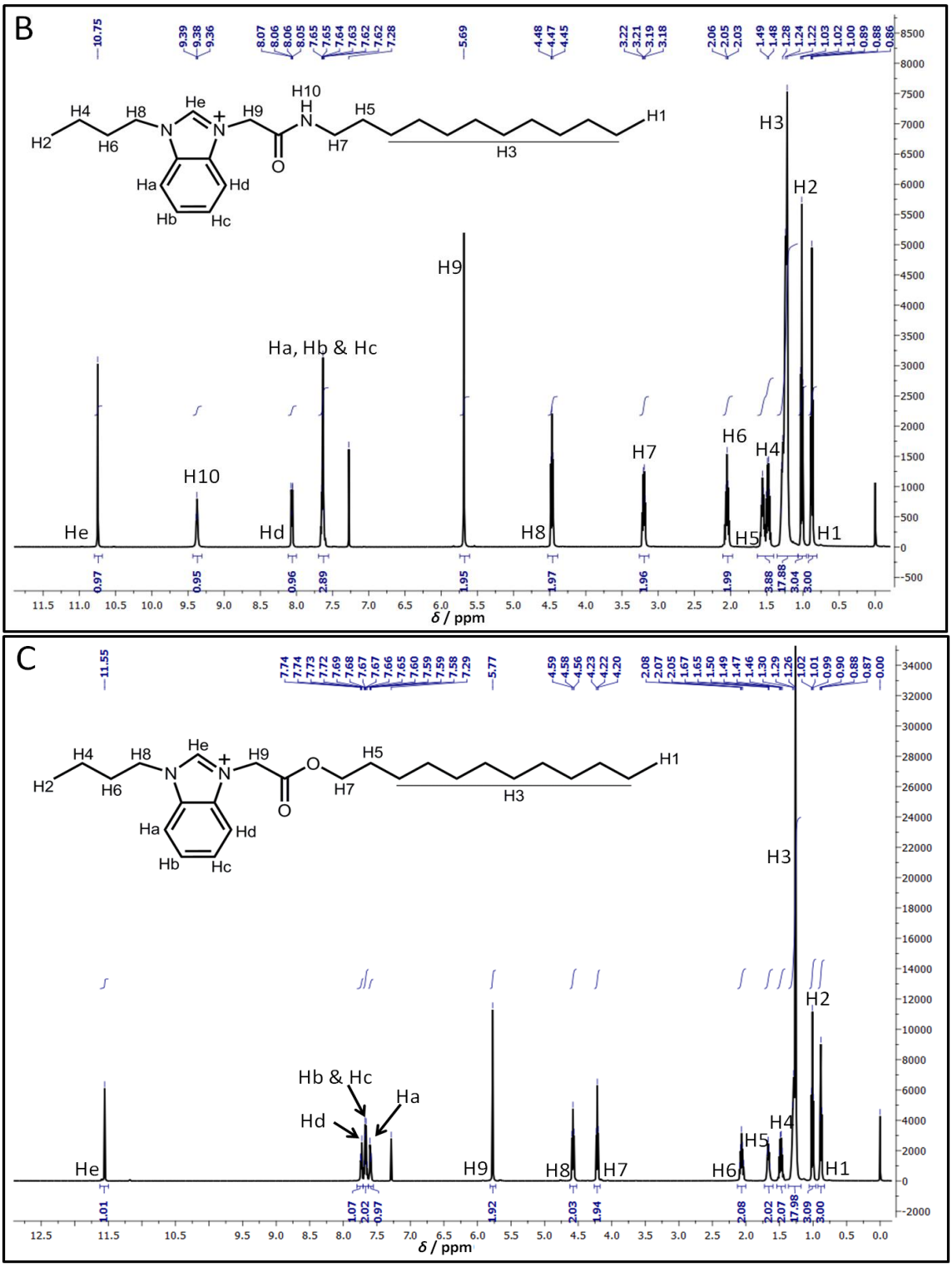

Fig. S2: Labeled ^{1}H NMR spectra of the three SAILs (A) [C_4C_{12}bzm][Cl]; (B) [C_4C_{12}Abzm][Cl] and (C) [C_4C_{12}Ebzm][Cl] along with their molecular structures.

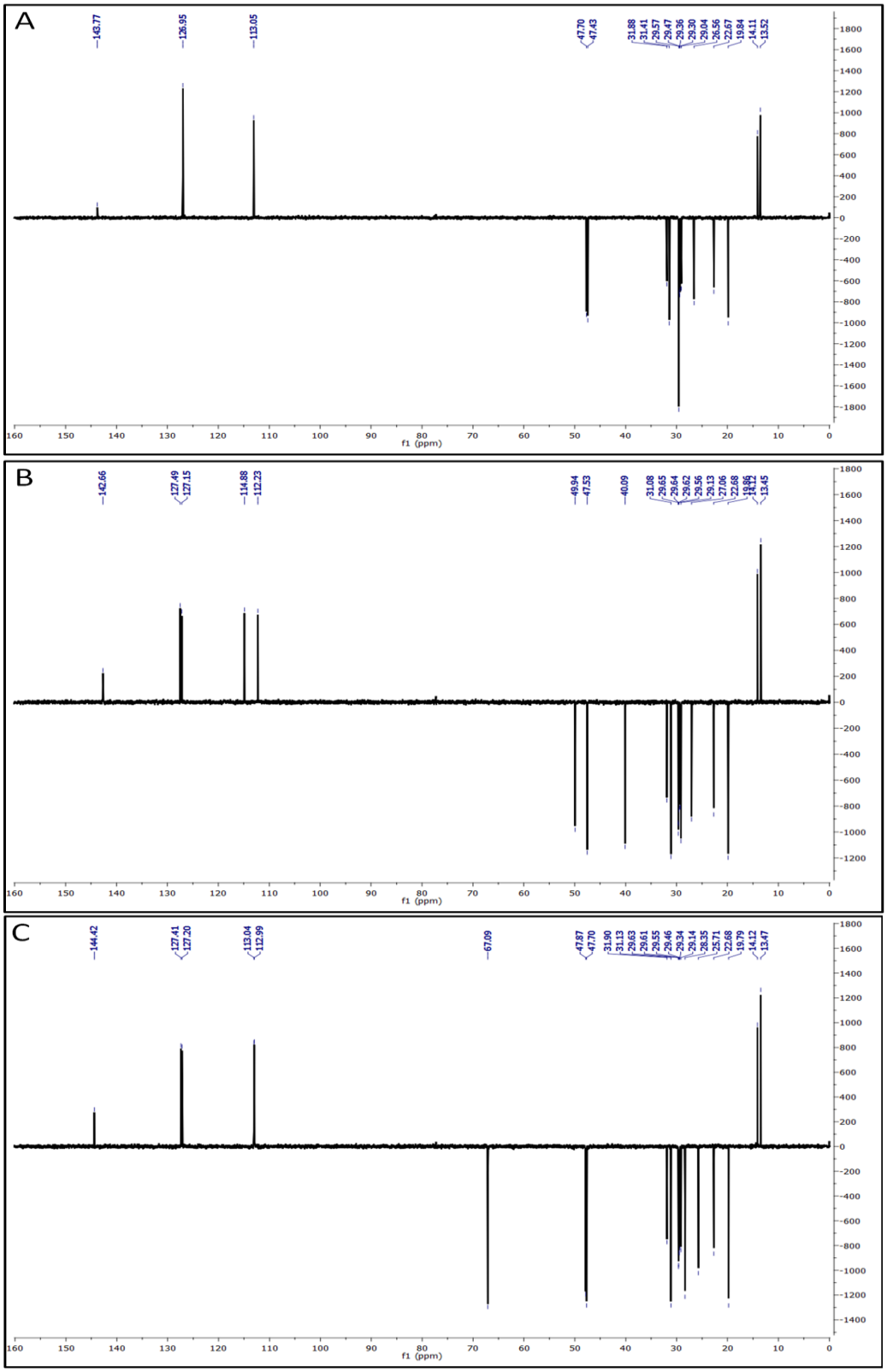

Fig. S3: ^{13}C/DEPT NMR spectra of the three SAILs (A) [C_4C_{12}bzm][Cl]; (B) [C_4C_{12}Abzm][Cl] and (C) [C_4C_{12}Ebzm][Cl].

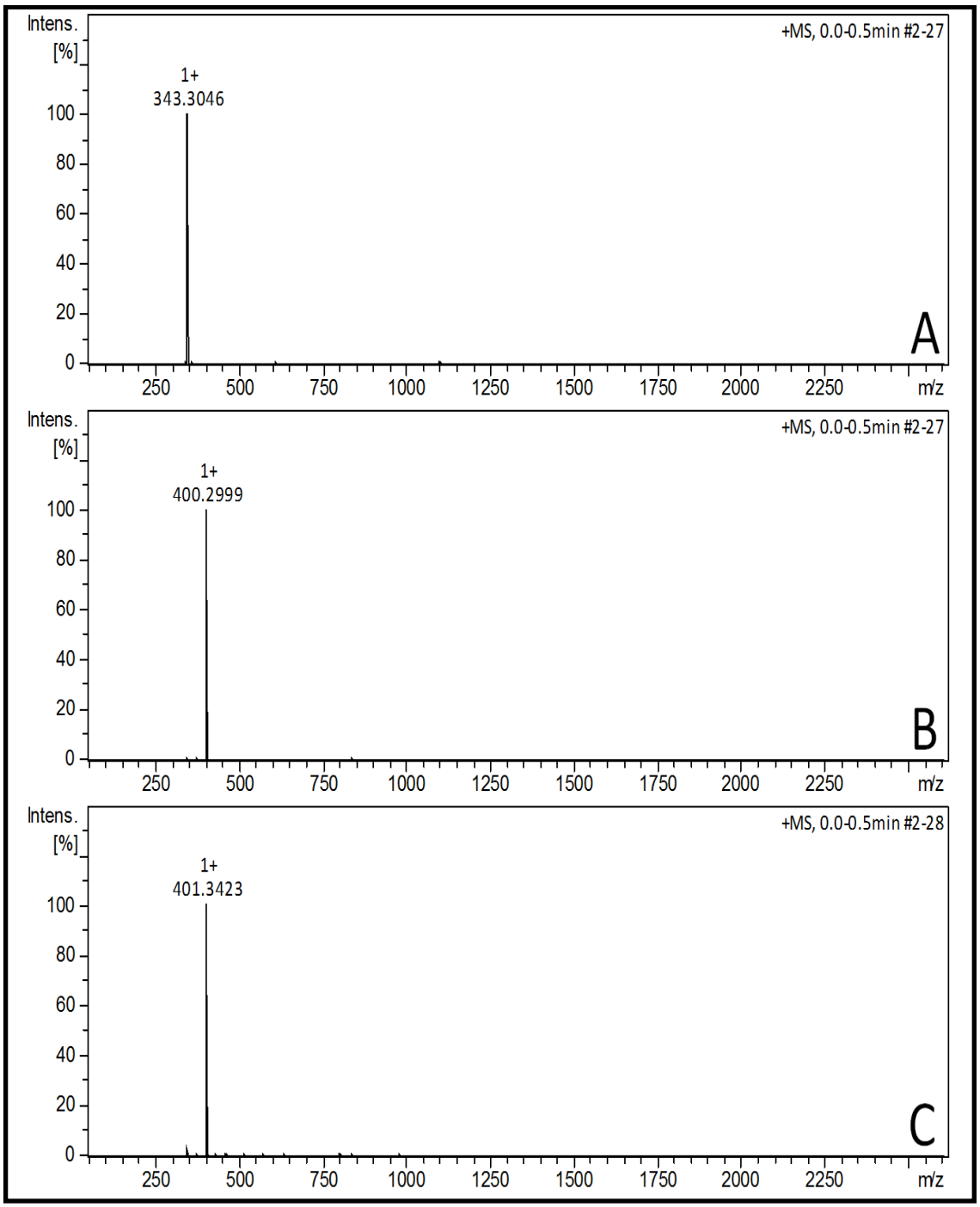

Fig. S4: HRMS spectra of the three SAILs (A) [C_4C_{12}bzm][Cl]; (B) [C_4C_{12}Abzm][Cl] and (C) [C_4C_{12}Ebzm][Cl].

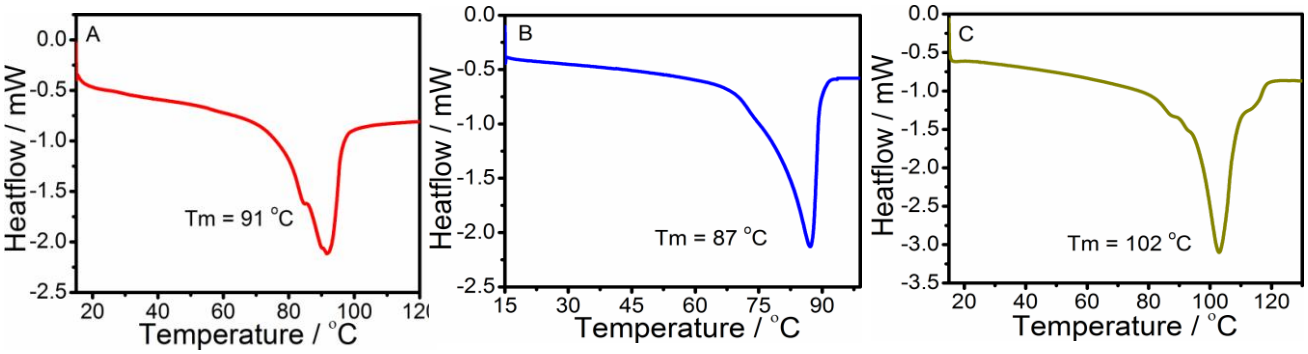

Fig. S5(A-C): Differential Scanning Calorimetry curves of (A)[C_4C_{12}bzm][Cl]; (B)[C_4C_{12}Abzm][Cl]; (C) [C_4C_{12}Ebzm][Cl] of the SAILs under investigation depicting their corresponding melting points (Tm).

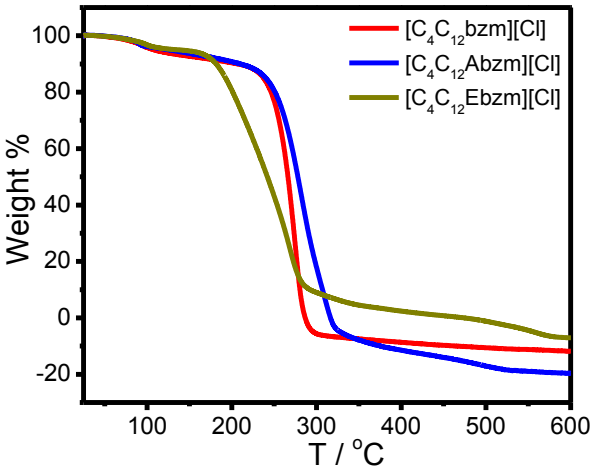

Fig. S6: Thermal gravimetric analysis (TGA) curves of the SAILs under investigation.

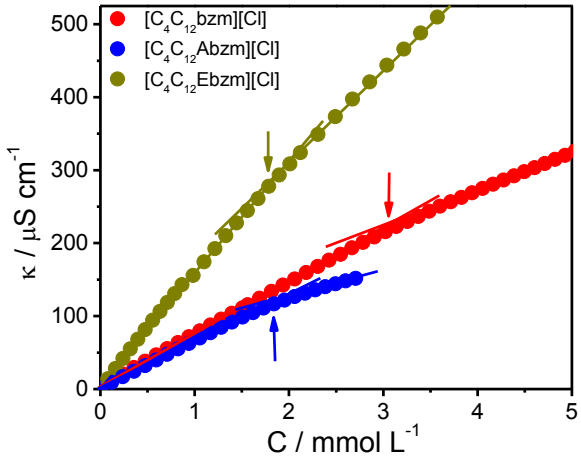

Fig. S7: Variation of specific conductance in aqueous solutions of the SAILs under investigation. The *cac* of respective ionic liquids has been marked by the arrows.

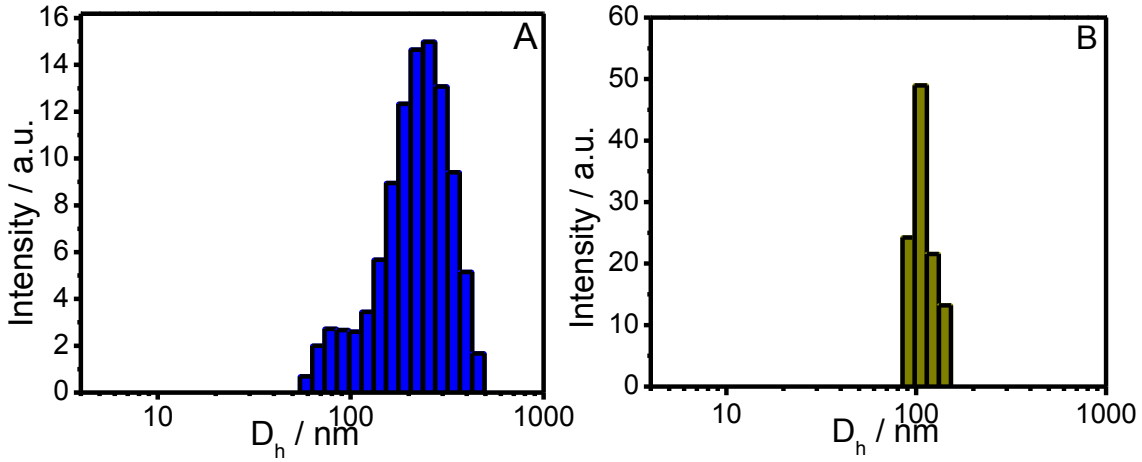

Fig. S8 (A-B): Intensity weighted size distribution of aqueous solutions of (A)[C_4C_{12}Abzm][Cl]; (B) [C_4C_{12}Ebzm][Cl] at a concentration twice the *cac* of respective ILs.

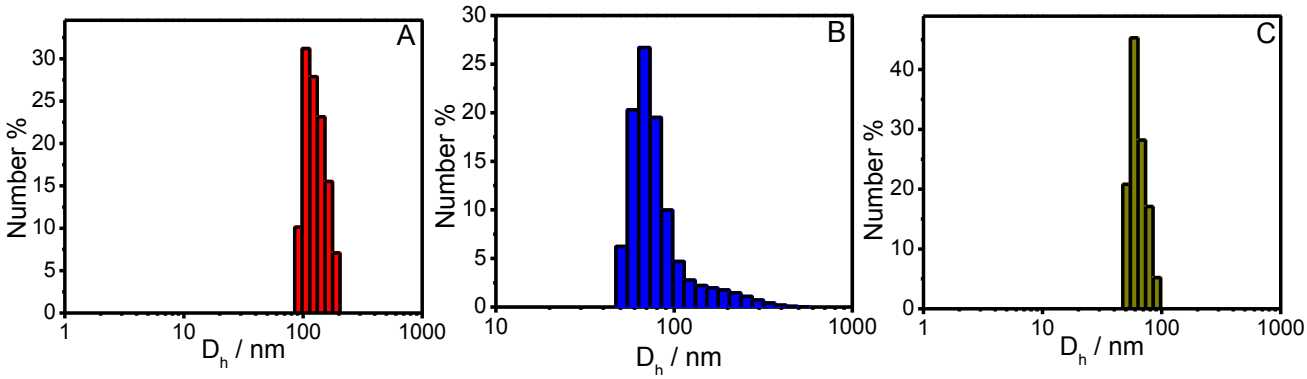

Fig. S9(A-C): Number average size distribution of aqueous solutions of (A)[C_4C_{12}bzm][Cl]; (B)[C_4C_{12}Abzm][Cl]; (C) [C_4C_{12}Ebzm][Cl] at a concentration twice the *cac* of respective SAILs.

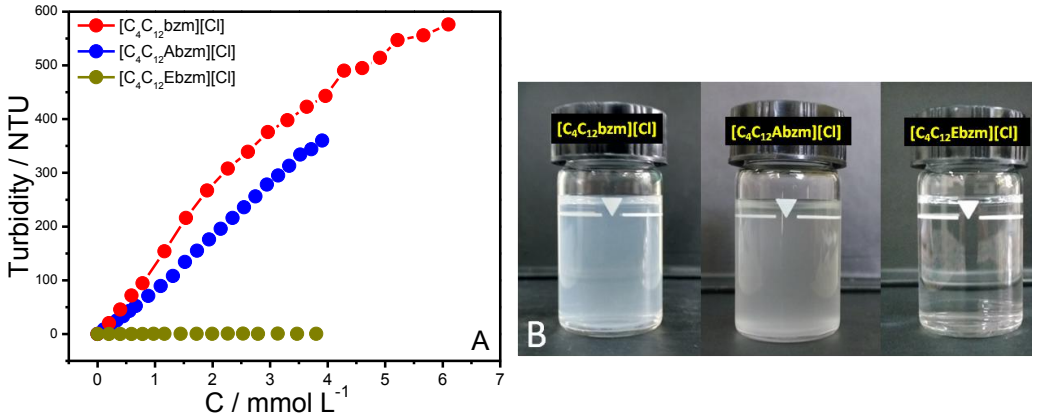

Fig. S10(A-B): (A) Variation in the turbidity of aqueous solutions of SAILs with increase in their concentration at 25^{o}C. (B) Image showing the translucence nature of the solutions of respective SAILs at twice their *cac* at 25^{o}C.

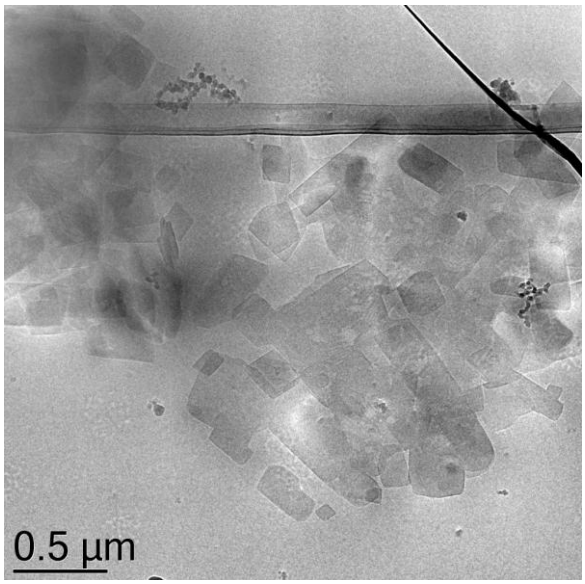

Fig. S11: Cryo-TEM image of 2D nano sheets formed by [C_4C_{12}bzm][Cl]. Nano sheets having different size range from 200-1500 nm has been captured in the image.

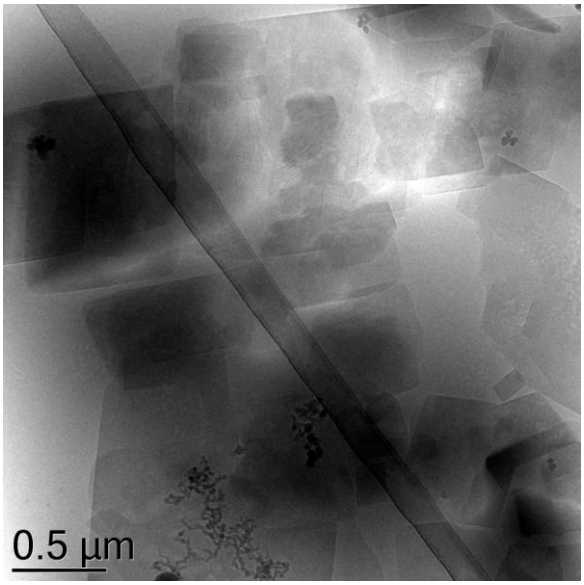

Fig. S12: Very thin 2D nano sheets formed by [C_4C_{12}bzm][Cl] lying beneath the other nano sheet can be seen in cryo-TEM image.

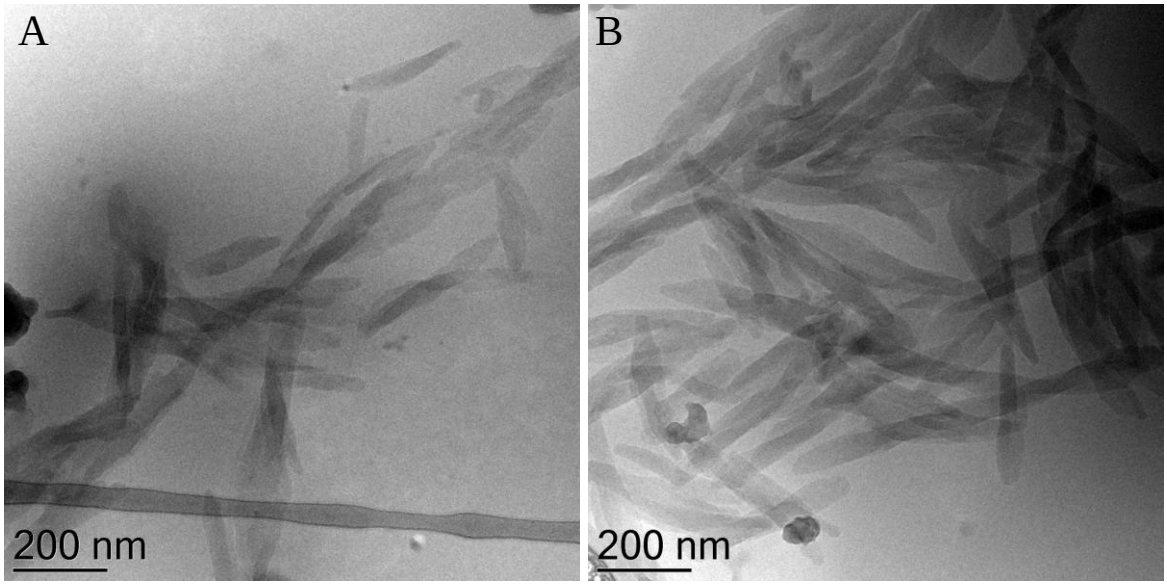

Fig. S13(A-B): (A) Cryo-TEM image of the very thin spindles lying beneath one another; (B) the twisted nature of the spindles formed by the twisting of bilayers of [C_4C_{12}Abzm][Cl].

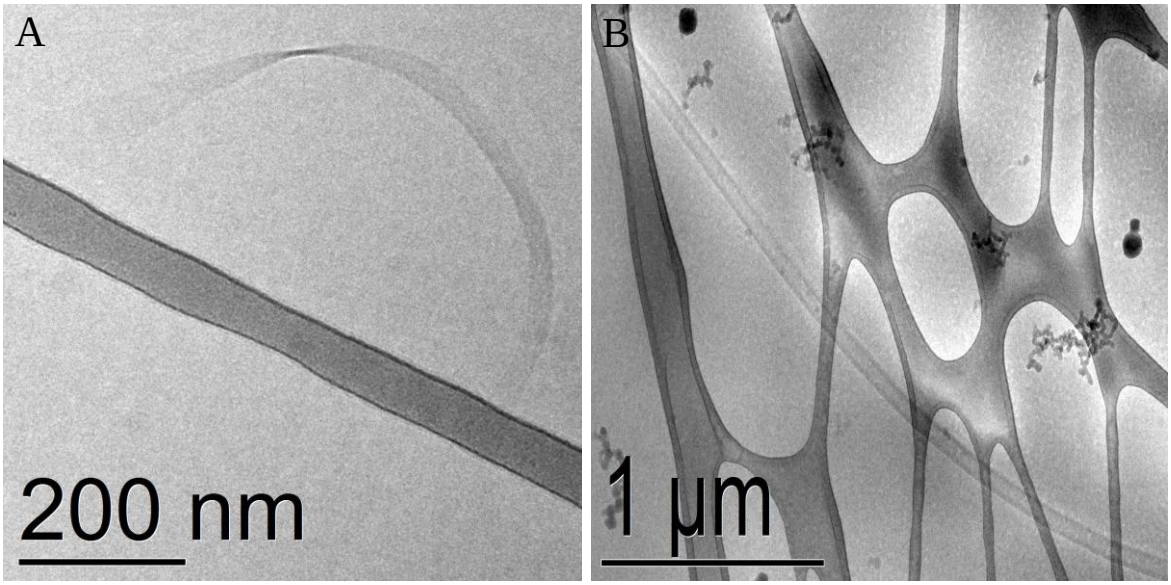

Fig. S14(A-B): (A) Cryo-TEM image of the very thin twisted ribbon; (B) very long flat ribbons formed from the bilayers of [C_4C_{12}Ebzm][Cl].

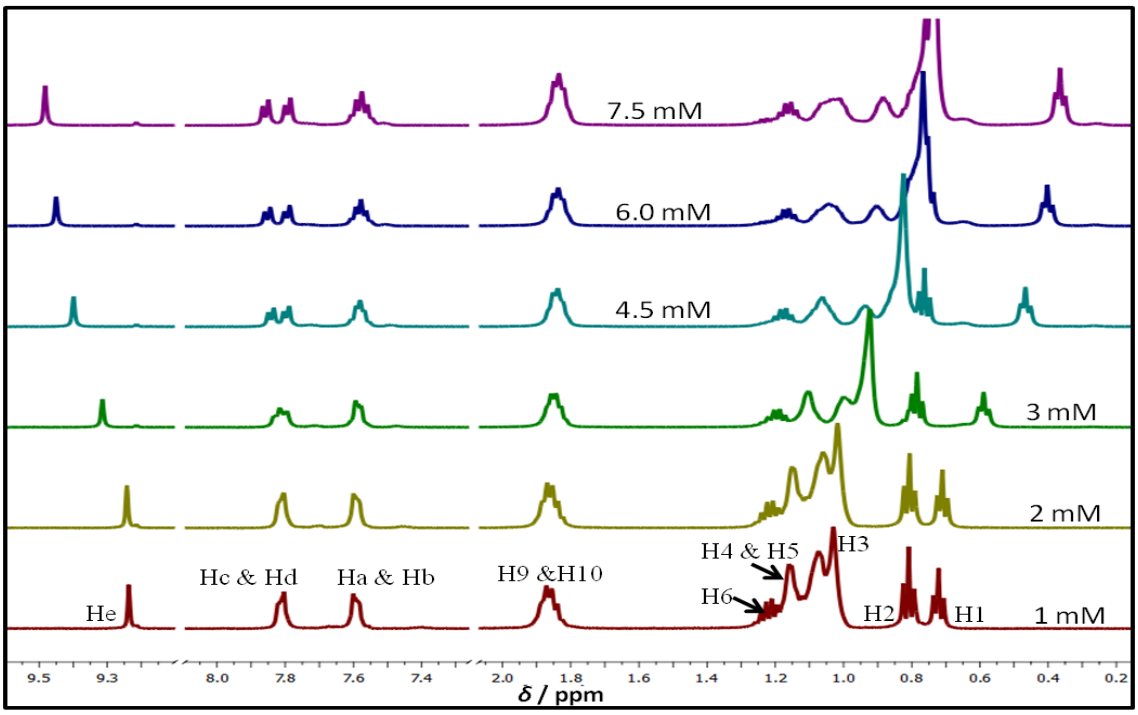

Fig. S15: Concentration dependent ^{1}H NMR spectra of [C_4C_{12}bzm][Cl] showing change in the chemical shift values of the various protons.

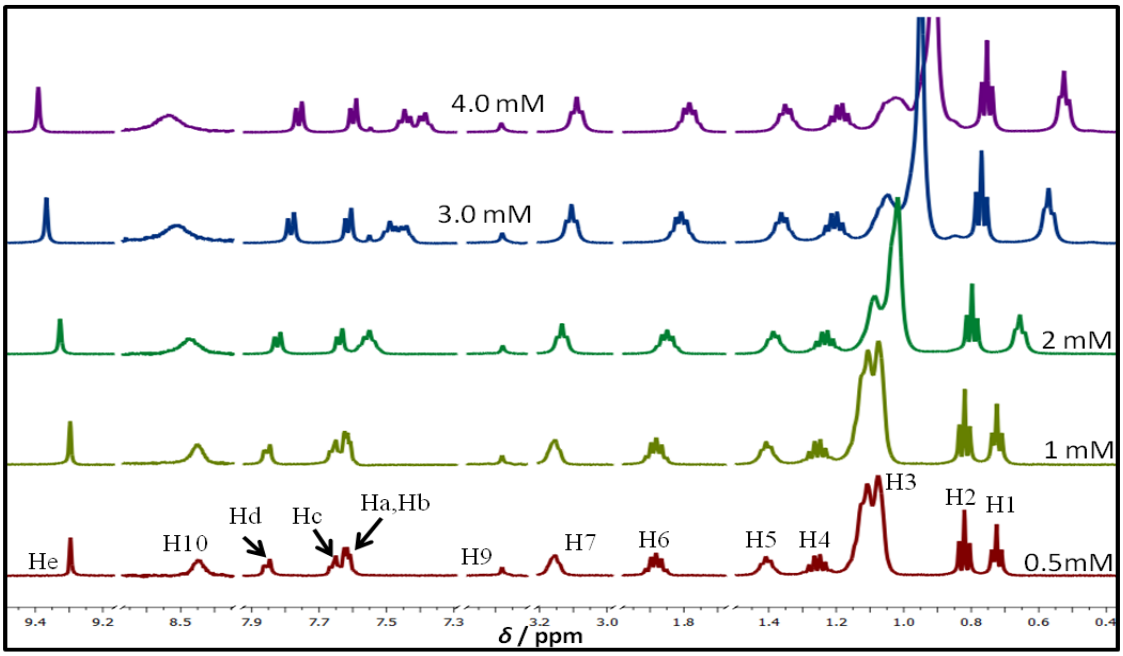

Fig. S16: Concentration dependent ^{1}H NMR spectra of [C_4C_{12}Abzm][Cl] showing change in the chemical shift values of the various protons.

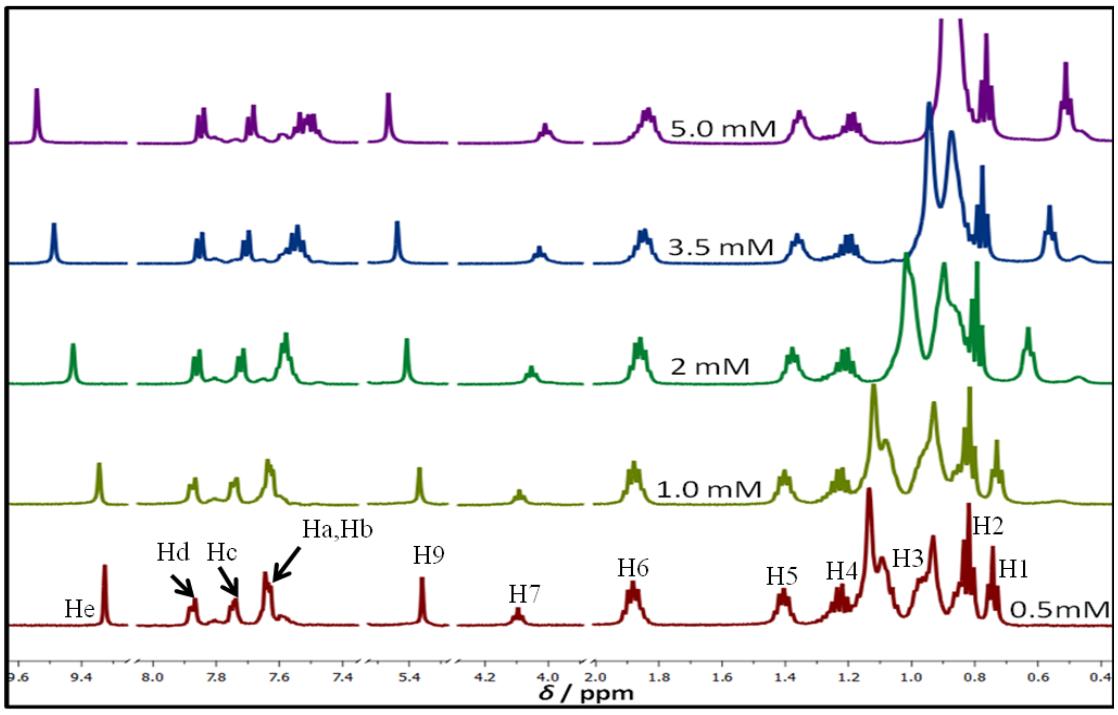

Fig. S17: Concentration dependent ^{1}H NMR spectra of [C_4C_{12}Ebzm][Cl] showing change in the chemical shift values of the various protons.

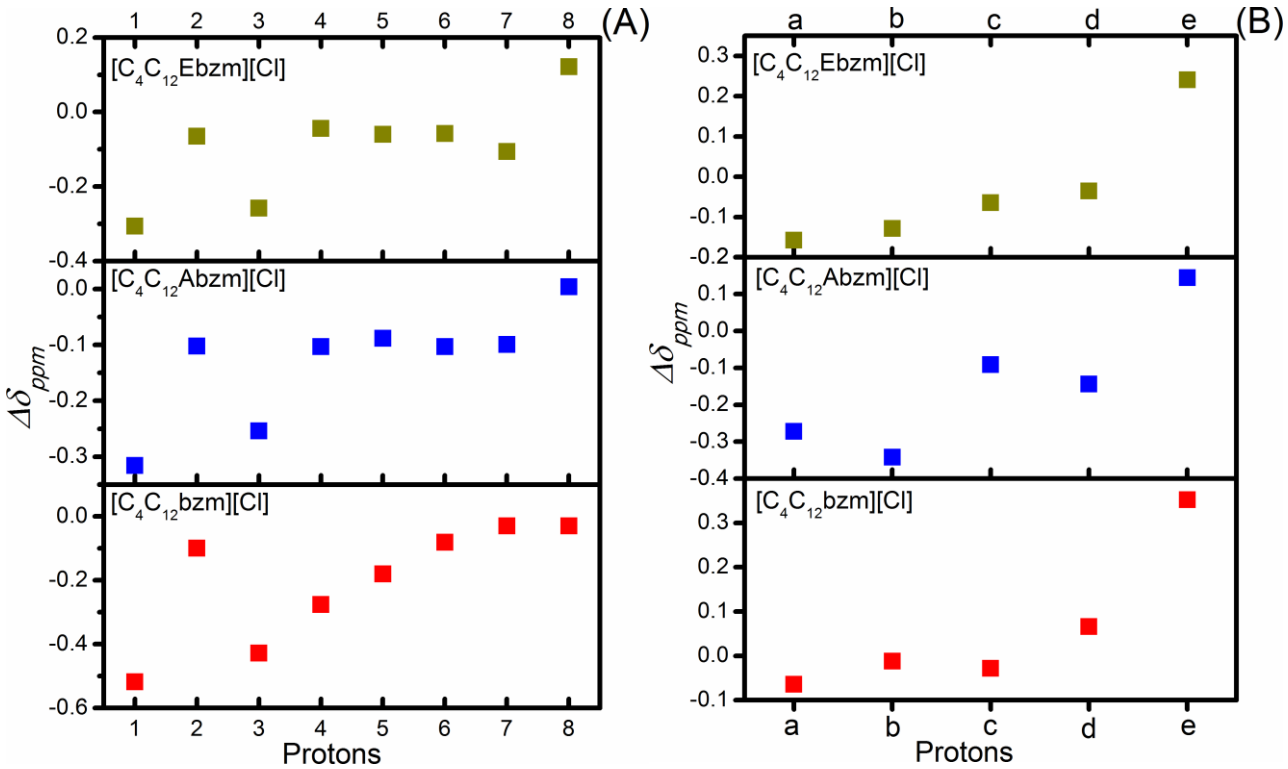

Fig. S18(A-B): (A) $\Delta\delta_{ppm}$ values for different protons of alkyl chain and butyl chain and **(B)** aromatic ring protons of the SAILs under investigation.

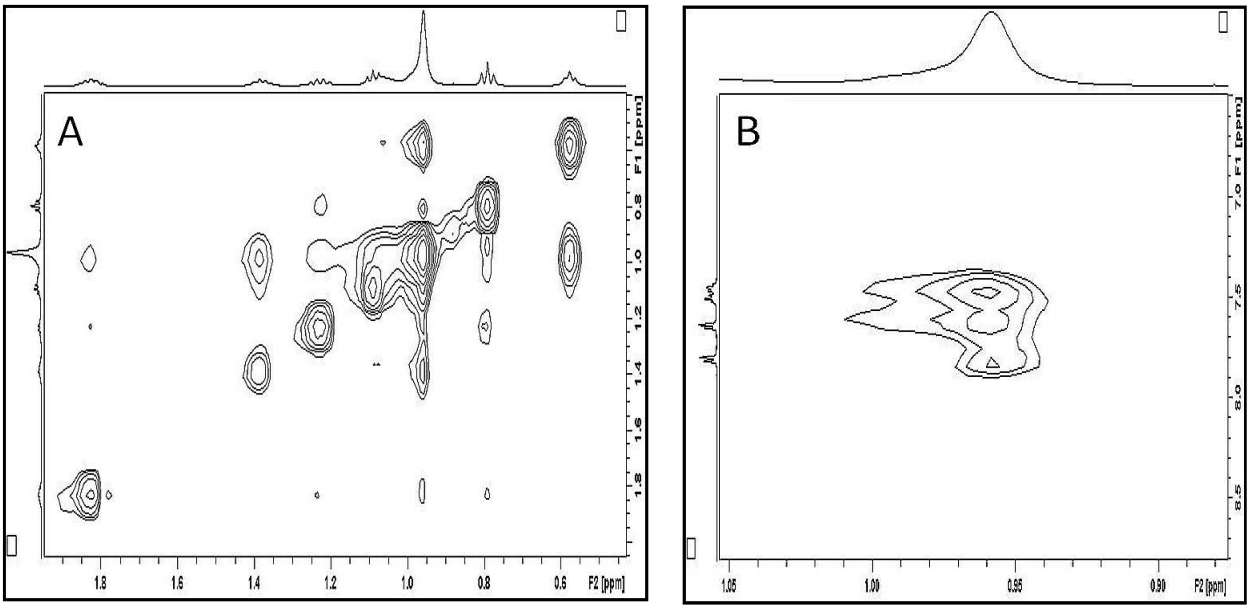

Fig. S19(A-B): (A) Enlarged view of the 2D ^{1}H-^{1}H NOESY spectra of [C_4C_{12}Abzm][Cl] in the region of alkyl chain protons **(B)** Cross peaks arising from the interaction of the alkyl chain protons and the aromatic protons of the benzimidazole ring.

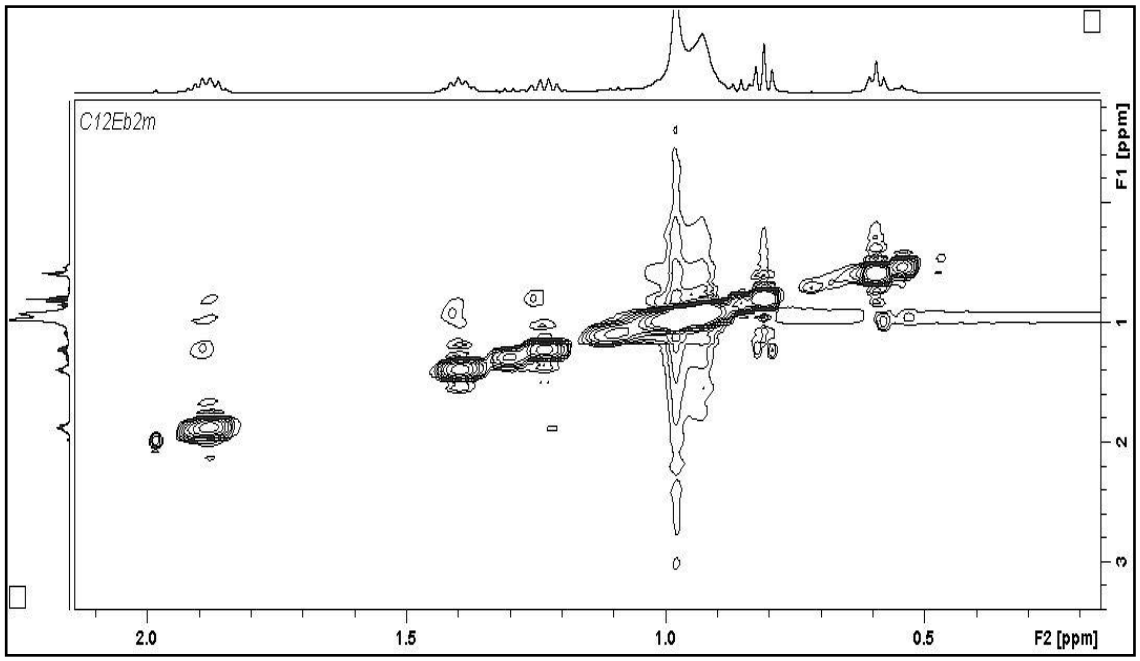

Fig. S20: Enlarged view of the 2D ^{1}H-^{1}H NOESY spectra of [C_4C_{12}Ebzm][Cl] in the region of alkyl chain protons showing a weak correlation between the protons.

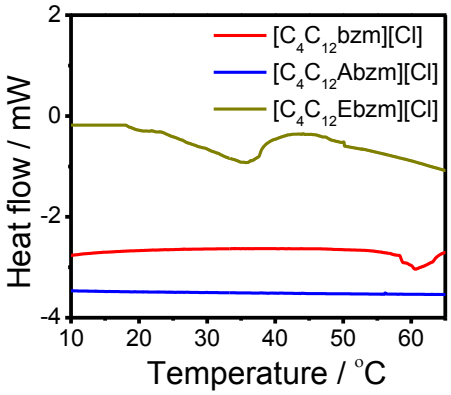

Fig. S21: Differential Scanning Calorimetry curves of respective SAILs at concentration twice their *cac* in the aqueous solutions.

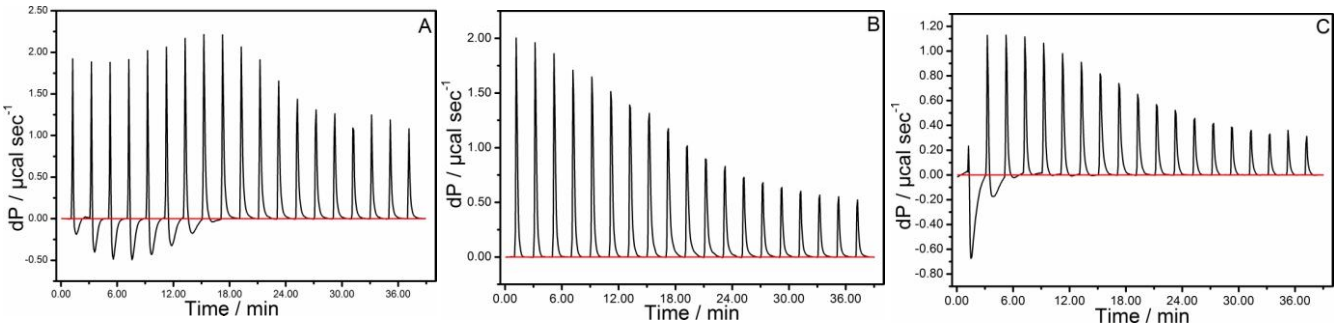

Fig. S22(A-C). Differential power (dP) profile obtained for the (A) $[C_4C_{12}bzm][Cl]$; (B) $[C_4C_{12}Abzm][Cl]$ and (C) $[C_4C_{12}Ebzm][Cl]$ in aqueous solutions at 298.15 K.

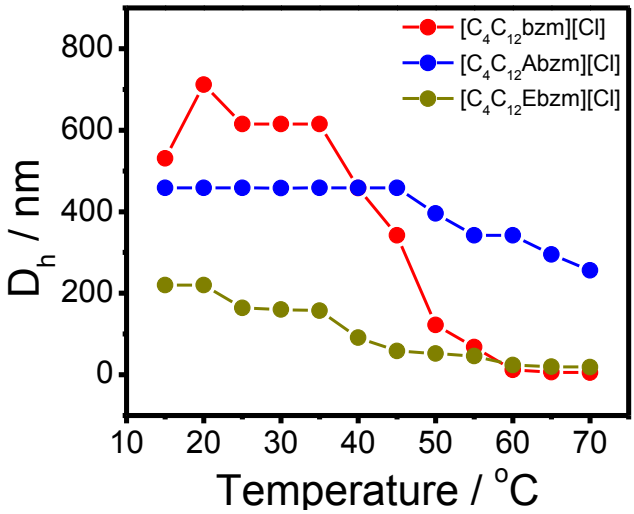

Fig. S23: Variation in the size of various aggregates formed by the respective SAILs in aqueous solution with the change in temperature.

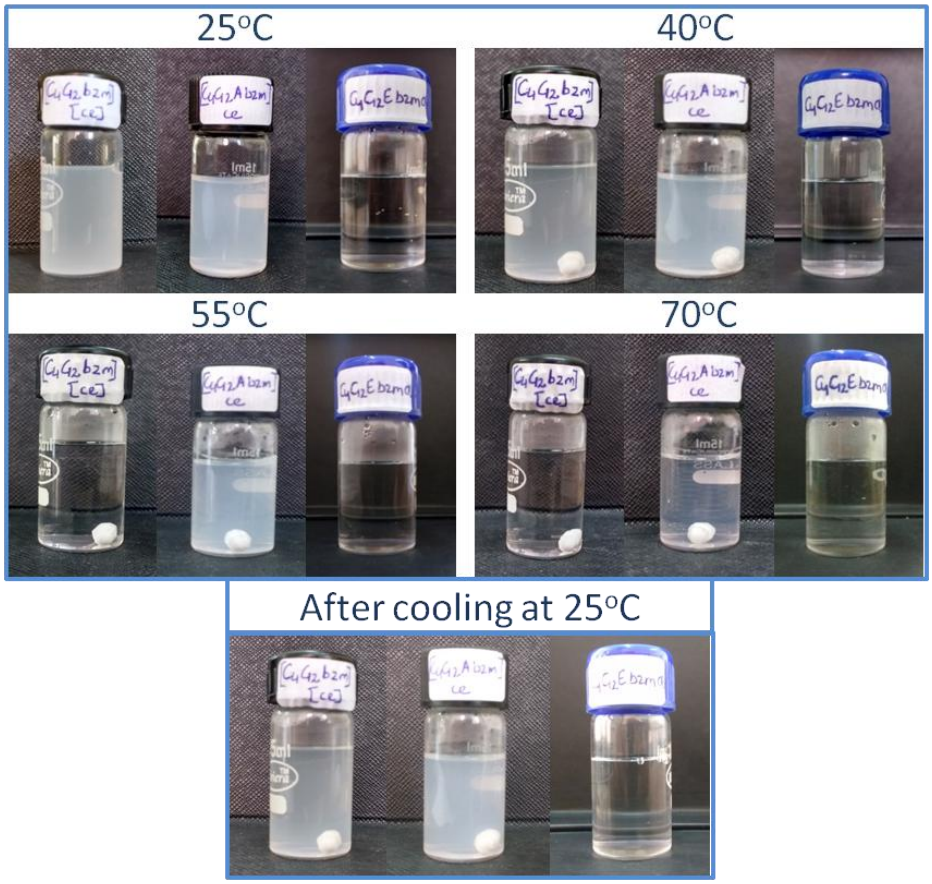

Fig. S24: Images of the aqueous solutions of SAILs under investigation at concentration twice their cmc values at different temperatures showing the change in the turbidity of solutions with change in temperature.

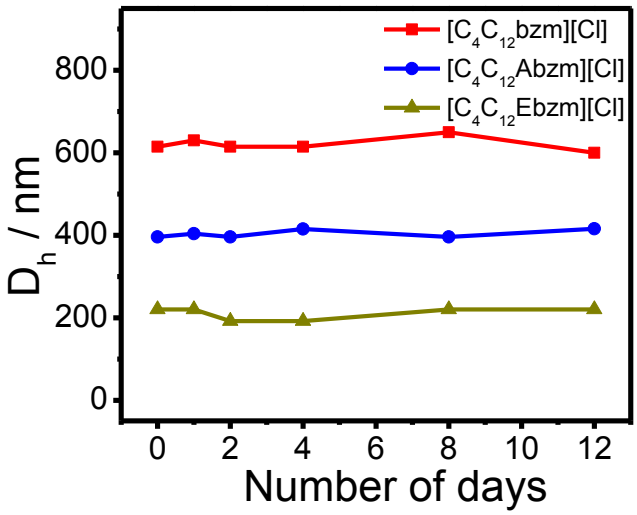

Fig. S25: Variation in the size of various aggregates formed by respective SAILs as a function of time showing the formation of stable aggregates.

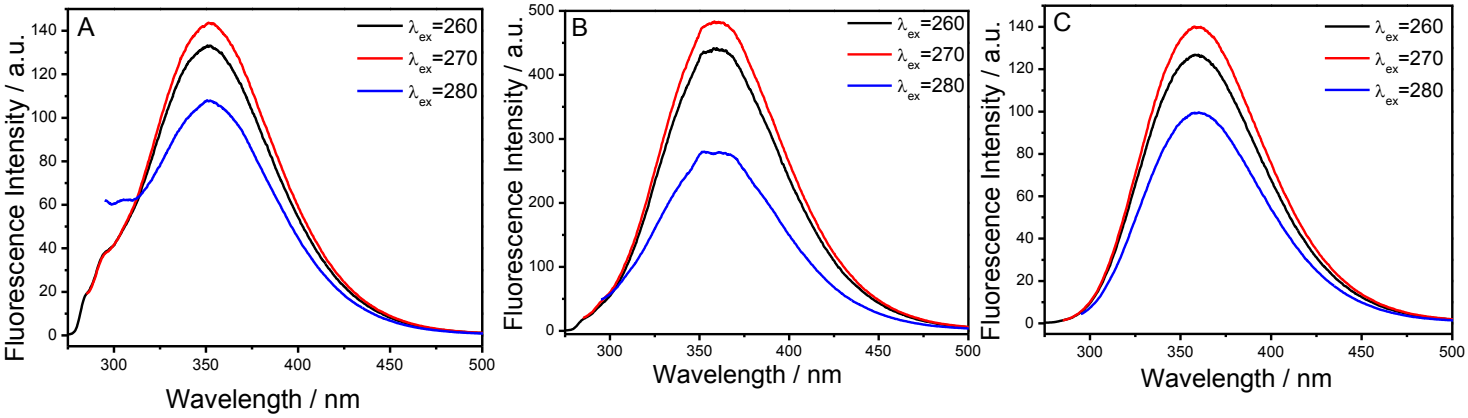

Fig. S26(A-B): Emission Spectra of aqueous solutions of respective SAILs (A) $[C_4C_{12}bzm][Cl]$; (B) $[C_4C_{12}Abzm][Cl]$ and (C) $[C_4C_{12}Ebzm][Cl]$ at different excitation wavelengths.

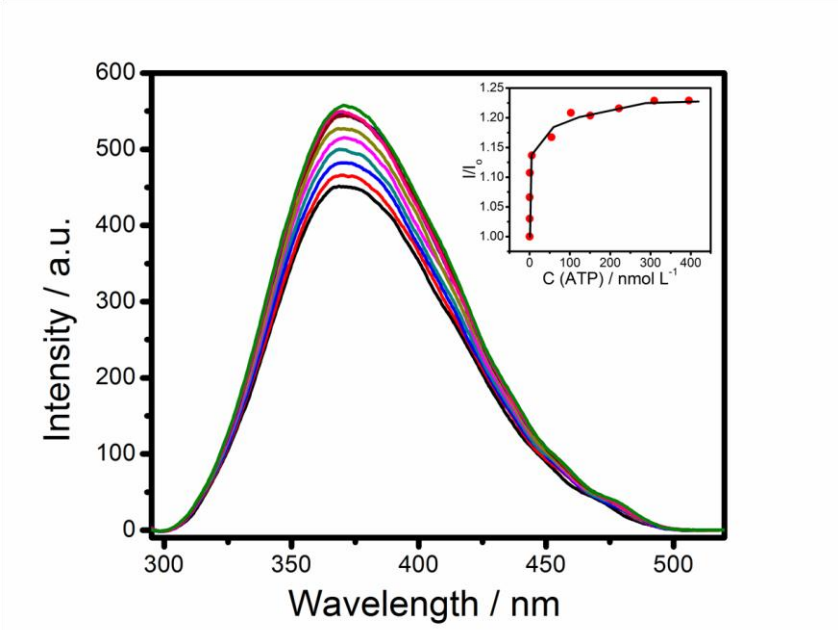

Fig. S27: Variation in the intensity emission spectra of $[C_4C_{12}Ebzm][Cl]$ in aqueous solutions with increase in the ATP concentration. Change in I/I_o values with increasing concentration of ATP has been shown in the inset.

Table S1. cac value from surface tension, conductivity and thermodynamic parameters obtained from the (ITC) value are listed.

SAIL	*ST*	*Cond.*	*ITC*		
	cac / mM		ΔG_m^o	ΔH_m^o	$T\Delta S_m^o$
$[C_4C_{12}bzm][Cl]$	1.40	3.10	-30.8	-0.65	30.15
$[C_4C_{12}Abzm][Cl]$	1.45	1.95	-35.9	-1.3	34.6
$[C_4C_{12}Ebzm][Cl]$	0.2	1.80	-31.6	-0.8	30.8

Units of ΔG_m^o, ΔH_m^o and $T\Delta S_m^o$ are kJ.mol^{-1}.

References:

1. O. Kose and S. Saito, *Org. Biomol. Chem.,* 2010, **8**, 896.
2. V. Chauhan, R. Kamboj, S. P. S. Rana, T. Kaur, G. Kaur, S. Singh and T. S. Kang, *J. Colloids Inter. Sci.,* 2015, **446**, 263.
3. R. Kamboj, P. Bharmoria, V. Chauhan, S. Singh, A. Kumar, V. S. Mithu and T. S. Kang, *Langmuir*, 2014, **30**, 9920.